

1 **Ebselen Reacts with SARS Coronavirus-2 Main Protease Crystals**

2 Tek Narsingh Malla¹, Suraj Pandey¹, Ishwor Poudyal¹, Denisse Feliz², Moraima Noda²,
3 George Phillips³, Emina Stojkovic², Marius Schmidt¹

4 University of Wisconsin-Milwaukee, Milwaukee, WI

5 Northeastern Illinois University, Chicago, IL

6 Rice University, Houston, TX

7

8 **Abstract.** The SARS coronavirus 2 main protease 3CLpro tailor cuts various essential virus
9 proteins out of long poly-protein translated from the virus RNA. If the 3CLpro is inhibited, the
10 functional virus proteins cannot form and the virus cannot replicate and assemble. Any compound
11 that inhibits the 3CLpro is therefore a potential drug to end the pandemic. Here we show that the
12 diffraction power of 3CLpro crystals is effectively destroyed by Ebselen. It appears that Ebselen
13 may be a widely available, relatively cost effective way to eliminate the SARS coronavirus 2.

14 **Introduction.**

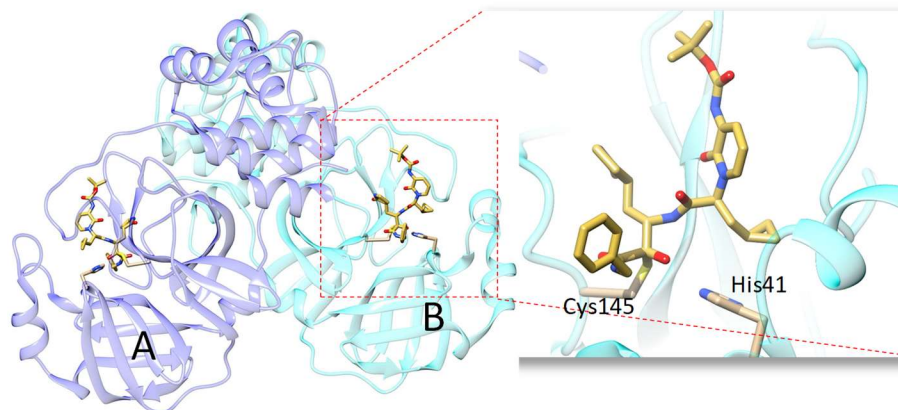
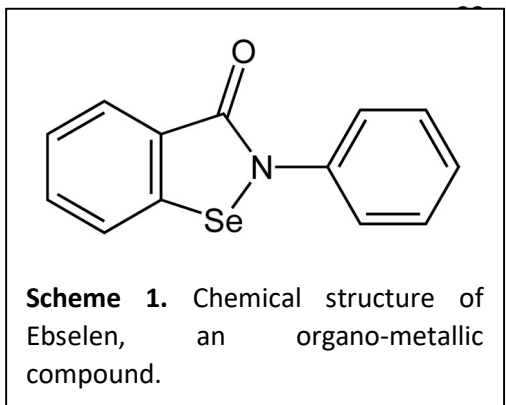


Figure 1. SARS CoV-2 3CLpro in its functional, dimeric form¹. The two subunits A and B are shown in dark and light blue. An α -ketoamide inhibitor is bound to the active site (red box, enlarged). The His-41/Cys-145 catalytic dyad is marked.

15 During the COVID-19 pandemic in the last half year, a large body of literature became available
16 to understand and combat the SARS coronavirus-2 (CoV-2). Due to its importance for virus protein
17 maturation the SARS CoV-2 main protease (Mpro), also called 3CLpro, became a major drug
18 target. In its functional form the 3CLpro is a homo dimer with His/Cys dyads (His-41 and Cys-
19 145) in the active centers¹. The structure of the CoV-2 3CLpro has been solved recently (Fig. 1)
20 guided by high similarity to other coronavirus 3CLpros¹. A large number (>500) of SARS CoV-2
21 3CLpro structures were recently deposited in the protein data bank mainly following a fragment
22 screening study at the synchrotron Diamond near Oxford, England. Binding of fragments not only
23 to the active center was observed. They all constitute a database of potential drugs to target the
24 3CLpro. Apart from the fragments, the most promising compounds are the α -ketoamides (Fig. 1)
25 which bind tightly to the 3CLpro¹⁻³. As they are complicated to synthesize they carry a hefty price

26 tag (companies ask for 14,000 dollars/g as recently inquired by one of the authors). A less
27 expensive, but also less known compound that binds to the 3CLpro is Ebselen⁴. Ebselen is a
28 selenium compound (Scheme 1) currently tested for a number of diseases such as bipolar disorder
29 and hearing loss⁴. Selenium is an essential metal, but toxic in higher doses. Ebselen has been shown
30 to bind strongly to the CoV-2 3CLpro⁴, but the structure of the complex is unknown. Here we
31 show what happens when Ebselen is added to 3CLpro crystals.

32 **Methods.**



Expression. The CoV-2 3CLpro sequence was synthesized (GenScript) for optimized expression in *E. coli* according to sequence information published previously¹. In short, the N-terminus of 3CLpro is fused to glutathione-S-transferase (GST). It further has a 6-His tag at the c-terminus. The N-terminal GST will be autocatalytically cleaved off after expression due to an engineered 3CLpro cleavage sequence. The His tag can be cleaved off by a PreCision Protease. Overexpression and protein purification protocols were modified from previous reports. *E. coli* were grown to 0.8 OD₆₀₀ at 37°

44 in terrific broth. Expression was induced by 1 mmol/L IPTG at 25° C. After 3 h of expression, the
45 culture was induced a second time (1 mmol/L IPTG), and shaken overnight at 20° C. The yield is
46 about 80 mg for a 6 L culture. Cells were resuspended in lysis buffer (20mM Tris Base, 150
47 mmol/L NaCl, pH 7.8.). After lysis of the bacterial cells, debris was centrifuged at 50,000 g for 1
48 hour. The lysate was let stand at room temperature for at least 3 h (overnight is also possible).
49 After this, the lysate was pumped through a column containing 15 mL of Talon Cobalt resin
50 (TAKARA). The resin was washed without using imidazole using a wash cycle consisting of low

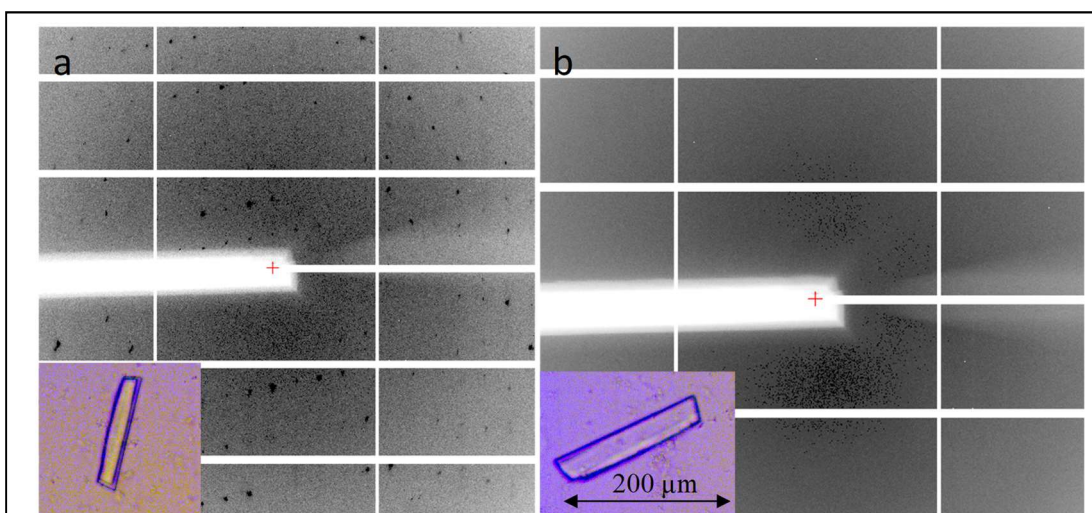


Figure 2. Low resolution (~3.5 Å in the corner) diffraction patterns of SARS CoV-2 3CLpro. (a) no ligand, (b) with Ebselen. Insets: crystal images w/o and w Ebselen, respectively

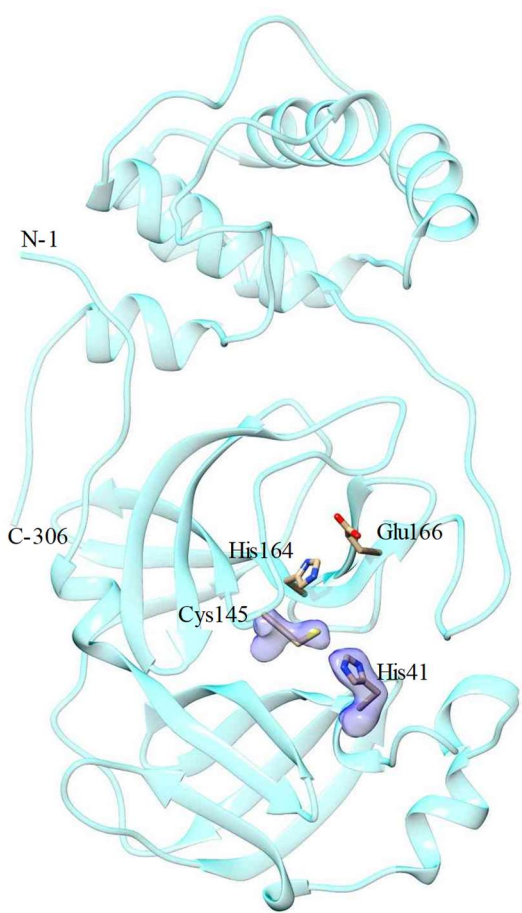


Figure 3. Structure of the SARS CoV-2 3CLpro without Ebselen as determined here. Electron density (1.2 sigma) is shown for the catalytic dyad. Other active site residues are also marked.

salt (20 mmol/L Tris Base, 50 mmol/L NaCl, pH 7.8), high salt (20 mmol/L Tris Base, 1 mol/L NaCl, pH 7.8) and low salt (as above) solutions (about 20 column volumes each). After the wash cycle was completed, the column was let stand for an additional 2 h at room temperature followed by another wash cycle. The final product was eluted by 300 mmol/L imidazole, dialyzed immediately in 20 mmol/L Tris base, 150 mmol/L NaCl, 0.1 mmol/L dithiotreitol (DTT), pH 7.8, and concentrated to 20 mg/mL. Note, the c-terminal 6-His tag was not cleaved off. Due to this one step purification protocol, only 24 h are required from cell lysis to the pure 3CLpro product. The product is within 1.7 Da of the theoretical molecular weight as determined by mass spectroscopy.

Crystallization. The concentrated 3CLpro (with the His-tag left on) was diluted to 4 mg/mL. 100 μ L of the diluted 3CLpro was mixed (1:1) in batch mode with the same amount of 25 % PEG 3350, Bis-Tris 100 mmol/L, pH 6.5. A few days later, nicely shaped crystals with dimensions of about 200 x 30 x 30 μ m³ were appearing. Crystals were soaked in mother liquor by adding Ebselen in powder form as Ebselen is not very soluble in water. Enough Ebselen that would otherwise produce a 50 mmol/L solution was added. After 2 days of soaking, the crystals

82 completely maintained their morphology (Fig. 2b).

83 *Data Collection and Structure determination.* The crystals were mounted in Mitegen microloops
84 (30 - 50 μ m) and directly frozen in pucks suspended in liquid nitrogen for automated (robotic) data
85 collection. The dewar with the pucks were driven to the Advanced Photon Source for robotic data
86 collection at Sector-19 (Structural Biology Center, SBC, beamline 19-ID-D). Data collection was
87 fully remote due to restriction of the COVID-19 pandemic. Fig. 2 shows a comparison of
88 diffraction patterns collected from untreated crystals (Fig. 2a), and crystals treated with the Ebselen
89 (Fig. 2b). As the untreated crystals diffracted beyond 2 \AA , the treated crystals did not show any
90 Bragg reflections whatsoever, even at lowest resolution. They are completely amorphous, despite
91 the nice crystal-like shape. Accordingly, the structure of only the untreated 3CLpro can be solved.
92 A dataset to 2.2 \AA was collected (0.5° rotation and 0.3 s exposure per detector readout for a total

93 of 180°). Data was processed with HKL3000⁵. Data statistics in shown in Tab. 1. Initially the
94 spacegroup was found to be C2 (monoclinic centered). It was further determined by the CCP4
95 program⁶ *pointless* that spacegroup I2 (monoclinic body centered) is more suitable, in accordance
96 with published results⁷. The 3CLpro structure with pdb access code 6WQF⁷ was used as initial
97 model. Molecular replacement was not necessary. The model fits immediately and can be used for
98 refinement. Refinement was done using refmac⁸ (version 5.8.0238). The structure is shown in Fig.
99 3. Its mean square deviation from model 6WQF is about 0.4 Å with 0.5 Å standard deviation. This
100 means that the 3CLpro cryo structure with the His-tag and the room temperature structure are
101 identical within the resolution limit. The structure of the His-tag could not be determined. There
102 is, however, a large crystal cavity near the C-terminus that might accommodate (a very disordered)
103 6 histidine structure.

104 **Results and Discussion.** A very important result is that c-terminal PreCission His-tag cleavage is
105 not required to obtain 3CLpro crystals. This speeds up purification to the extent that now gram
106 sized 3CLpro preparations can be obtained in a relatively short period of time. This is a prerequisite
107 for mix-and-inject approaches at free electron lasers with gas-dynamic-virtual-nozzle type mixing
108 injectors^{9,10}. At XFELs low concentrations of Ebselen can be mixed with the crystalline slurry
109 which is quickly injected into the X-ray beam. There is hope that crystal decomposition is slower
110 than the delay between mixing and injection. Then, the structure of the Ebselen-3CLpro complex
111 may be determined. In addition, microcrystals also tend to be unusually flexible and may survive
112 large unit cell changes¹¹, which might make these experiments even more conceivable.

113 Since Ebselen has this strong effect on 3CLpro crystals, it a clear indication for the tight affinity
114 of this compound to the 3CLpro. Binding of Ebselen to the catalytic dyad has been already
115 identified by mass-spectroscopy and published earlier⁴. However, also after the experiments
116 reported here, the 3CLpro-Ebselen structure remains elusive. As Ebselen is a potent drug (and it
117 is not too toxic even in higher concentrations⁴), it has to be seen whether it can be used as an
118 effective weapon against the SARS CoV-2, and maybe all other pathogenic coronaviruses.
119 Whether it is suitable for a drug must be determined by physicians in a clinical setting perhaps in
120 combination with a SARS CoV-2 RNA dependent RNA polymerase inhibitor such as remdesivir¹².
121 As crystallographers and structural biologists, though, we can deliver evidence for a potential
122 mechanism as shown recently by others for the α -ketoamides^{1,2} and also remdesivir¹².

123 This manuscript is published without delay on BioRxiv to disseminate rapid methods for
124 preparation, purification and structure determination of 3CLpro to a wide community. In addition,
125 this manuscript intends to alert and increase awareness of the potential of Ebselen as a 3CLpro
126 inhibitor and its value perhaps in combination, as the authors are not aware that anything is
127 reported about it in the public press. The coordinates of the 100 K 3CLpro structure as determined
128 here are available on request.

129 **Acknowledgement.** This work is supported by NSF grant STC 1727290 (BioXFEL) and NSF
130 grant RAPID 2030466. Results shown in this report are derived from work performed at Argonne
131 National Laboratory (ANL), Structural Biology Center (SBC) at the Advanced Photon Source
132 (APS), under U.S. Department of Energy, Office of Biological and Environmental Research

133 contract DE-AC02-06CH11357. The authors thank Darren A. Sherrell for setting up the
134 experiment at the beamline.

135

136 **Table. 1** Data collection and refinement statistics*

137

	SARS CoV-2 3CLpro
Beamline	19-ID-D, APS
Resolution	2.2 Å
Temperature	110 K
Space group	I2
Unit-cell parameters (,°)	$a = 44.7 \text{ \AA}$ $b = 53.4 \text{ \AA}$ $c = 112.3 \text{ \AA}$ $\alpha = 90^\circ$ $\beta = 100.0^\circ$ $\gamma = 90^\circ$
No of unique reflections	9426
Redundancy	3.1 (1.9)
Completeness (%)	70.0
CC1/2 (%)	99.8 (47.6)
R_{merge} (%)	7.3 (76.5)
Refinement	
$R_{\text{cryst}}/R_{\text{free}}$ (%)	19.1/26.3
RMSD to 6WQF ⁷	0.39 +/- 0.53 Å

138

*last resolution shell in brackets

139 **References.**

140 1 Zhang, L. L. *et al.* Crystal structure of SARS-CoV-2 main protease provides a basis for
141 design of improved alpha-ketoamide inhibitors. *Science* **368**, 409-+.

142 2 Zhang, L. L. *et al.* alpha-Ketoamides as Broad-Spectrum Inhibitors of Coronavirus and
143 Enterovirus Replication: Structure-Based Design, Synthesis, and Activity Assessment.
144 *Journal of Medicinal Chemistry* **63**, 4562-4578.

145 3 Dai, W. *et al.* Structure-based design of antiviral drug candidates targeting the SARS-
146 CoV-2 main protease. *Science* **368**, 1331-1335, PMC7179937.

147 4 Jin, Z. M. *et al.* Structure of M-pro from SARS-CoV-2 and discovery of its inhibitors.
148 *Nature* **582**, 289-+.

149 5 Minor, W., Cymborowski, M., Otwinowski, Z. & Chruszcz, M. HKL-3000: the
150 integration of data reduction and structure solution - from diffraction images to an initial
151 model in minutes. *Acta Crystallographica Section D-Structural Biology* **62**, 859-866.

152 6 Winn, M. D. *et al.* Overview of the CCP4 suite and current developments. *Acta
153 Crystallogr D* **67**, 235-242.

154 7 Kneller, D. W. *et al.* Structural plasticity of SARS-CoV-2 3CL M-pro active site cavity
155 revealed by room temperature X-ray crystallography. *Nat Commun* **11**.

156 8 Murshudov, G. N. *et al.* REFMAC5 for the refinement of macromolecular crystal
157 structures. *Acta crystallographica. Section D, Biological crystallography* **67**, 355-367,
158 3069751.

159 9 Olmos, J. L., Jr. *et al.* Enzyme intermediates captured "on the fly" by mix-and-inject
160 serial crystallography. *BMC Biol* **16**, 59, PMC5977757.

161 10 Calvey, G. D., Katz, A. M. & Pollack, L. Microfluidic Mixing Injector Holder Enables
162 Routine Structural Enzymology Measurements with Mix-and-Inject Serial
163 Crystallography Using X-ray Free Electron Lasers. *Anal Chem* **91**, 7139-7144.

164 11 Stagno, J. R. *et al.* Structures of riboswitch RNA reaction states by mix-and-inject XFEL
165 serial crystallography. *Nature* **541**, 242-246.

166 12 Yin, W. C. *et al.* Structural basis for inhibition of the RNA-dependent RNA polymerase
167 from SARS-CoV-2 by remdesivir. *Science* **368**, 1499-+.

168